# Signal sequence insufficiency contributes to neurodegeneration caused by transmembrane prion protein

Neena S. Rane,[1] Oishee Chakrabarti,[1] Lionel Feigenbaum,[2] and Ramanujan S. Hegde[1]

[1]Cell Biology and Metabolism Program, National Institute of Child Health and Human Development, National Institutes of Health, Bethesda, MD 20892
[2]Laboratory of Animal Sciences, National Cancer Institute, Frederick, MD 21702

Protein translocation into the endoplasmic reticulum is mediated by signal sequences that vary widely in primary structure. In vitro studies suggest that such signal sequence variations may correspond to subtly different functional properties. Whether comparable functional differences exist in vivo and are of sufficient magnitude to impact organism physiology is unknown. Here, we investigate this issue by analyzing in transgenic mice the impact of signal sequence efficiency for mammalian prion protein (PrP). We find that replacement of the average efficiency signal sequence of PrP with more efficient signals rescues mice from neurodegeneration caused by otherwise pathogenic PrP mutants in a downstream hydrophobic domain (HD). This effect is explained by the demonstration that efficient signal sequence function precludes generation of a cytosolically exposed, disease-causing transmembrane form of PrP mediated by the HD mutants. Thus, signal sequences are functionally nonequivalent in vivo, with intrinsic inefficiency of the native PrP signal being required for pathogenesis of a subset of disease-causing PrP mutations.

## Introduction

N-terminal signal sequences are essential for the translocation of nearly all secretory proteins across the mammalian ER (Rapoport, 2007). After cotranslational recognition by the signal recognition particle, signal-bearing proteins are targeted to ER translocons composed of the Sec61 protein-conducting channel. The signal sequence then gates open the Sec61 channel to initiate translocation of the nascent polypeptide across the ER membrane. The sequence requirements for a signal to carry out these critical steps in translocation are remarkably flexible, needing only a hydrophobic core of ~7–9 residues (von Heijne, 1985). For this reason, it was long thought that sequence diversity among natural signals represents degeneracy in functional requirements.

In recent years, however, there is growing appreciation that substrate-specific differences among signal sequences may have functional consequences (Martoglio and Dobberstein, 1998; Hegde and Bernstein, 2006). For example, analyses in biochemical and cell culture systems suggests that signals may differ in their gating of the Sec61 translocon (Rutkowski et al., 2001; Kim et al., 2002), dependence on accessory translocation factors (Voigt et al., 1996; Fons et al., 2003), overall efficiency in mediating translocation (Belin et al., 1996; Levine et al., 2005; Shaffer et al., 2005), or sensitivity to translocation inhibitors (Besemer et al., 2005; Garrison et al., 2005). Even native proteins have been observed to generate small nontranslocated populations in the cytosol in a signal sequence–dependent manner (Rane et al., 2004; Shaffer et al., 2005; Kang et al., 2006). Thus, signals from different proteins may not be as functionally uniform as generally assumed. However, the in vivo relevance of these slight and variable differences in efficiency among signal sequences is poorly studied.

A key issue is whether a native signal-containing protein, synthesized in its appropriate cell types in vivo, ever displays any appreciable inefficiency in order to generate a biologically relevant nontranslocated population. This question is difficult to address for several reasons. First, the nontranslocated species

Correspondence to Ramanujan S. Hegde: hegder@mail.nih.gov

Abbreviations used in this paper: cyPrP, cytosolic PrP; GD, globular domain; GFAP, glial fibrillary acidic protein; HD, hydrophobic domain; Opn, osteopontin; PK, proteinase K; Prl, prolactin; PrP, prion protein.



The Rockefeller University Press $30.00
J. Cell Biol.
www.jcb.org/cgi/doi/10.1083/jcb.200911115

Supplemental Material can be found at:
http://jcb.rupress.org/cgi/content/full/jcb.200911115/DC1

would presumably be of very low abundance, representing a few percent of total synthesized protein. Second, nontranslocated species are likely to be very transient because of their rapid degradation by quality control pathways. Third, in vivo systems are largely inaccessible to the same analytical tools typically used in vitro and in cell culture. Thus, direct and reliable detection of nontranslocated species or direct assays to measure signal sequence efficiencies in vivo are exceedingly difficult.

These problems of detection can be circumvented if any nontranslocated polypeptides can either be trapped or have measurable and sensitive downstream consequences. Fortuitously, certain disease-causing prion protein (PrP) mutants meet these requirements and afford a unique opportunity to test whether in vivo signal sequences display either appreciable inefficiency or functional differences. Mammalian PrP, which is causative of various neurodegenerative diseases (Prusiner et al., 1998), contains a typical ER signal sequence of apparently average efficiency (Kim et al., 2002). The normal and primary outcome of PrP biosynthesis at the ER is its complete translocation into the lumen, where the N-terminal signal sequence is removed, two consensus sites become glycosylated, and a C-terminal peptide is processed to a glycosylphosphatidylinositol anchor (Fig. 1, A and B). However, PrP polypeptides whose signals fail to initiate translocation have two possible outcomes depending on downstream sequence elements (Kim et al., 2001; Kim and Hegde, 2002; Stewart and Harris, 2003). The first outcome is the release of PrP into the cytosol, where it is rapidly degraded by a proteasome-dependent pathway. Hence, proteasome inhibition permits nontranslocated PrP to accumulate (Ma and Lindquist, 2001; Yedidia et al., 2001; Drisaldi et al., 2003), an event that can be prevented by a more efficient signal sequence (Rane et al., 2004). The second outcome is production of a transmembrane isoform of PrP termed $^{Ctm}$PrP. This occurs when a highly conserved downstream hydrophobic domain (HD) engages the translocon before PrP is released to the cytosol (Kim and Hegde, 2002). In vitro, both of these outcomes are detectable and can be modulated in a predictable fashion by changing the properties of the signal sequence and HD (Kim et al., 2001, 2002; Kim and Hegde, 2002; Stewart and Harris, 2003). Thus, both $^{Ctm}$PrP and cytosolic PrP (cyPrP) appear to be products of signal sequence inefficiency.

Although cyPrP is very difficult to detect in vivo because of its rapid proteasomal degradation, $^{Ctm}$PrP seems to be significantly more stable (Stewart and Harris, 2005). This means that $^{Ctm}$PrP represents a "trapped" product of failed translocation. Thus, when hydrophobicity of the HD is increased, signal sequence inefficiency results in generation of $^{Ctm}$PrP (Kim et al., 2001). Because $^{Ctm}$PrP levels are correlated with neurodegeneration in mice (Hegde et al., 1998a, 1999; Stewart et al., 2005), we reasoned that it should be possible to measure differences in signal efficiency in the context of a whole organism. Our strategy was to determine if $^{Ctm}$PrP (and the ensuing neurodegeneration) caused by an HD mutant could be rescued by changing the signal sequence to one that, based on in vitro studies, should be more efficient. This experiment was designed to address four inter-related questions of relevance to protein translocation and PrP biology. First, are native signal sequences sufficiently

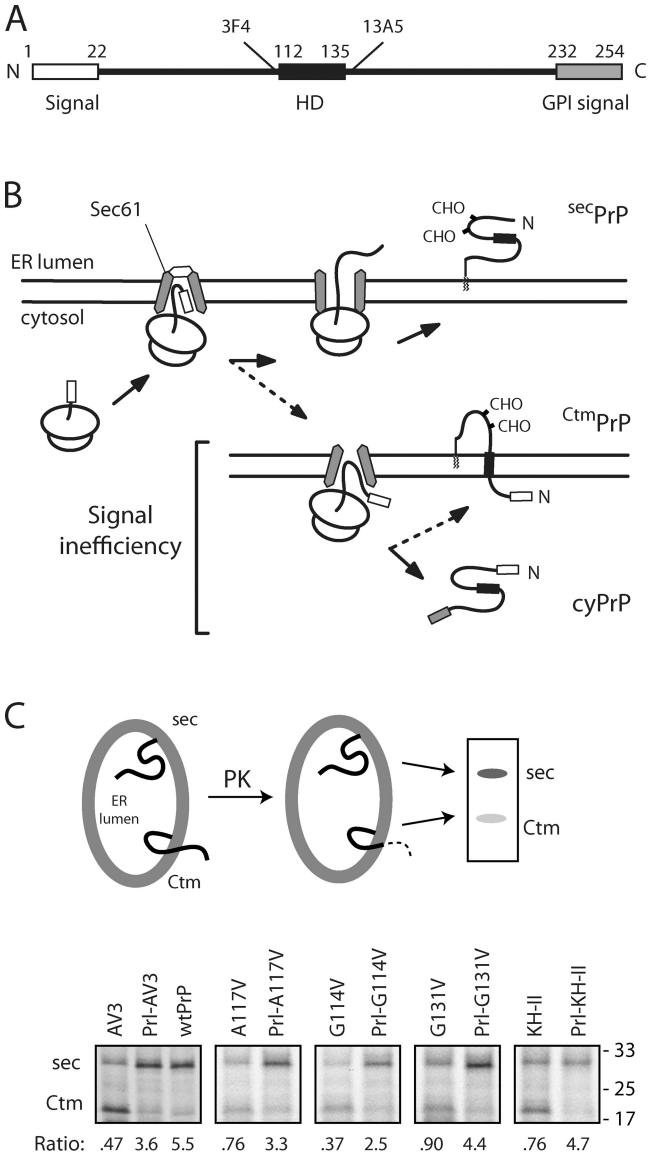


Figure 1. **Improving signal efficiency reduces $^{Ctm}$PrP in vitro.** (A) Line diagram of PrP showing elements involved in its translocation. Amino acid residues of key domains, and the epitopes for the 3F4 and 13A5 monoclonal antibodies, are indicated. (B) Steps in PrP translocation. Starting at the left, PrP is targeted to a Sec61 translocon via its N-terminal signal sequence. The signal then interacts with Sec61 and gates open the channel to initiate translocation. Further protein synthesis results in complete translocation into the ER lumen to generate $^{sec}$PrP. This is the normal pathway followed by the majority of PrP polypeptides synthesized. However, intrinsic inefficiencies in the signal sequence interaction with the translocon can cause a small proportion of PrP polypeptides to fail at the crucial gating/initiation steps. The bottom shows the two potential outcomes when signal-mediated gating and/or early translocation fails. In the first case, the polypeptide is expelled into the cytosol to generate cyPrP. Alternatively, the central HD, particularly if it carries a mutation that increases hydrophobicity, can engage the nearby translocon to generate $^{Ctm}$PrP. (C) Analysis of translocation and topology of various PrP constructs in vitro. The indicated constructs were translated in reticulocyte lysate containing rough microsomes. The samples were then digested with PK and analyzed by SDS-PAGE and autoradiography. The diagram illustrates the assay whereby $^{sec}$PrP is fully protected from PK digestion, whereas $^{Ctm}$PrP is partially digested to generate an 18-kD fragment. The ratio of the $^{sec}$PrP to $^{Ctm}$PrP products for each construct is shown below the individual lanes. Note that each of the mutations increases $^{Ctm}$PrP (i.e., reduced sec/Ctm ratio) but is largely reverted when the signal sequence from Prl is used. Numbers to the right indicate molecular mass in kD.

different in function in vivo to impact normal physiology? Second, is the native PrP signal sequence detectably inefficient in vivo? Third, are the in vitro mechanistic models of PrP translocation and $^{Ctm}$PrP production valid in vivo? Fourth, do HD mutations cause disease via $^{Ctm}$PrP production, or do they have another previously unforeseen effect?

## Results

### Effect of signal sequence efficiency on $^{Ctm}$PrP production in vitro

Several natural and artificial disease-associated PrP mutations within the HD were analyzed for $^{Ctm}$PrP generation in vitro using a reticulocyte lysate translation system containing pancreatic rough microsomes. The assay for PrP topology in vitro is based on protease protection and has been described previously (Hegde et al., 1998a; Fig. S1 A). In brief, protease treatment of PrP translocation reactions causes $^{Ctm}$PrP to be partially digested, fully translocated PrP to be completely protected, and nontranslocated PrP to be completely digested. The ratio of fully protected PrP (operationally termed $^{sec}$PrP to indicate its full translocation like a secretory protein) to the $^{Ctm}$PrP-derived fragment is therefore an indicator of how much ER-targeted PrP is generated in the $^{Ctm}$PrP form. This sec/Ctm ratio was used to assess the PrP mutants.

PrP(A117V), PrP(G114V), and PrP(G131V) are each natural point mutants in human PrP that increase HD hydrophobicity and are associated with the neurodegenerative disease Gerstmann-Sträussler-Schienker Syndrome (Tateishi et al., 1990; Hsiao et al., 1991; Panegyres et al., 2001; Rodriguez et al., 2005). Of these, rodent PrPs containing the A117V mutation have been expressed in transgenic mice and shown to cause neurodegeneration (Hegde et al., 1998a; Yang et al., 2009). PrP(AV3) is an artificial mutant in rodent PrP that contains three alanine-to-valine changes within the HD, substantially increases HD hydrophobicity, and causes early onset neurodegeneration upon expression in transgenic mice (Hegde et al., 1998a). PrP(KH-II) is a different type of artificial mutant in rodent PrP that lengthens the HD toward the N terminus and presumably shifts slightly the residues that would span the bilayer. This too causes neurodegeneration in transgenic mice (Hegde et al., 1998a, 1999). As expected, each of these HD mutations, when analyzed in vitro, generates increased $^{Ctm}$PrP relative to wild-type PrP (Fig. 1 C). Hence, although wild-type PrP has a sec/Ctm ratio of 5.5, each of the HD mutants shows ratios of <1.

Based on earlier studies of PrP translocation (Kim and Hegde, 2002), increased $^{Ctm}$PrP results from PrP molecules that would have failed to be translocated because of an inefficient signal sequence, but now insert into the membrane because the mutant HD can better engage the translocon (Fig. 1 B). Consistent with this mechanism, the effect of hydrophobic HD mutants was largely reversed in vitro by replacing the somewhat inefficient PrP signal sequence with the highly efficient signal from the secretory protein prolactin (Prl; Fig. 1 C). This is apparent by the more than fourfold increase in the sec/Ctm ratio for each HD mutant that brings it close, but not quite equal, to wild-type levels. This suggests that $^{Ctm}$PrP generation by HD mutants in vitro depends on signal sequence inefficiency. Furthermore, $^{Ctm}$PrP levels can be substantially normalized back toward wild-type levels by the Prl signal sequence. It is worth noting that the absolute sec/Ctm ratio values vary somewhat between different batches of translation extracts and microsomes (for example, compare Fig. 1 C to Fig. S1 A). This is presumably because there are trans-acting factors in both the cytosol (Lopez et al., 1990) and membrane (Hegde et al., 1998b; Fons et al., 2003), whose activities can vary and influence translocation and topology of PrP. Nonetheless, the key observations that HD mutants increase $^{Ctm}$PrP relative to wild type, and that the Prl signal sequence largely normalizes $^{Ctm}$PrP of HD mutants back toward normal, are consistently observed.

Analysis of wild-type PrP in cultured cells indicates that the amount of nontranslocated cyPrP is ∼10% of total PrP synthesized (Rane et al., 2004), with unknown (but assumed to be low) levels of $^{Ctm}$PrP. This level of signal inefficiency is also consistent with estimates derived from artificial reporter assays of signal function in mammalian cultured cells (Levine et al., 2005). This suggests that the PrP signal is indeed partially inefficient in cells, as seen in vitro. To determine whether this inefficiency plays a role in $^{Ctm}$PrP production, we turned to a previously characterized limited protease digestion assay that can discriminate $^{Ctm}$PrP from other forms by virtue of its slightly different conformation (Hegde et al., 1998a, 1999).

Under the digestion conditions used, properly folded nontransmembrane PrP forms are trimmed at the unstructured N terminus (up to residue ∼125), leaving behind an intact C-terminal globular domain (GD) that presumably corresponds to the core structure seen in nuclear magnetic resonance studies (Riek et al., 1996, 1997; Donne et al., 1997). In contrast, $^{Ctm}$PrP is digested to only residue ∼105, apparently because the membrane-inserted HD acquires a different conformation that is retained even after detergent solubilization. Thus, the resulting fragment from $^{Ctm}$PrP (∼18 kD) is slightly larger than the core GD (∼15 kD). The 3F4 monoclonal antibody, whose epitope falls within residues ∼109–112, selectively recognizes the $^{Ctm}$PrP fragment and is therefore invaluable for this assay. The amount of the $^{Ctm}$PrP fragment detected by 3F4 can be quantified by comparing to serial dilutions of undigested total lysate. Notably, some HD mutants within or near the 3F4 epitope (such as KH-II) interfere with 3F4 antibody binding and therefore must be detected by other C-terminal antibodies that detect both $^{Ctm}$PrP and GD fragments. As a practical matter, this somewhat limits assay sensitivity because the two fragments migrate closely, proteolysis is not absolutely precise (resulting in some fragment heterogeneity), and the $^{Ctm}$PrP fragment is vastly less abundant than the GD fragment.

Using this assay, $^{Ctm}$PrP levels in transiently transfected cultured cells expressing wild-type PrP were determined to be <1–2% (Fig. 2). This suggests that the wild-type HD does not engage the translocon with high efficiency in cells. In contrast, HD mutants detectably increase $^{Ctm}$PrP levels (Fig. 2). The most hydrophobic artificial HD mutants PrP(AV3) and PrP(KH-II) were roughly equivalent, each producing ∼10% $^{Ctm}$PrP (Fig. 2). As expected, PrP(A117V) generated an intermediate level of ∼4% $^{Ctm}$PrP. The increased $^{Ctm}$PrP seen with PrP(AV3) was reduced to near wild-type levels when the native PrP signal and cleavage site were replaced with the corresponding region from Prl (a construct

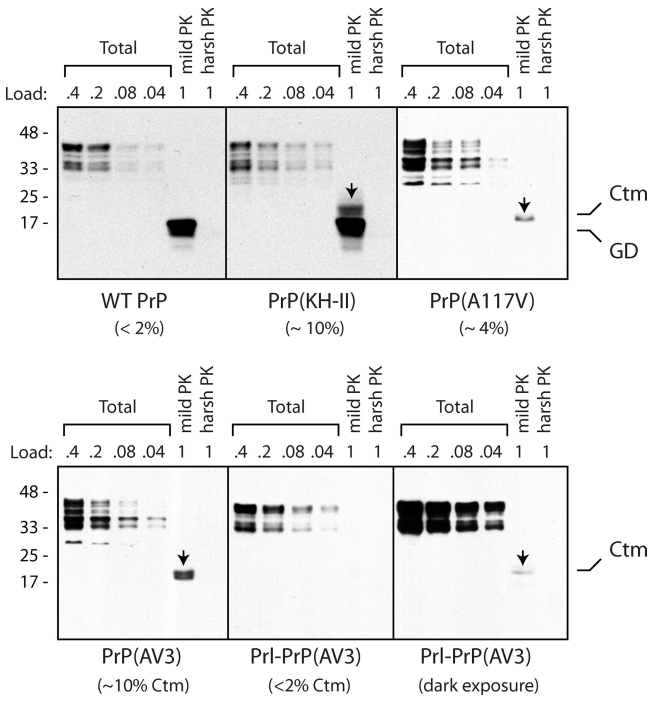


Figure 2. **Analysis of PrP translocation and $^{Ctm}$PrP in cultured cells.** Limited PK digestion assay for $^{Ctm}$PrP in crude microsomes isolated from N2a cells transfected with the indicated constructs. Samples were subjected to PK digestion under either mild or harsh conditions (as described in Materials and methods). The protease-digested samples were deglycosylated with peptide-*N*-glycosidase F and analyzed by immunoblotting alongside serial dilutions of untreated samples (first four lanes of each panel). The relative amounts loaded in each lane are indicated above the gels. Blots were probed with monoclonal antibodies 13A5 (wild-type [WT] and KH-II panels) or 3F4 (other panels). The $^{Ctm}$PrP-specific fragment (arrows) and C-terminal GD fragment (recognized only by the 13A5 antibody) are indicated. The percentage of total PrP in the $^{Ctm}$PrP form was quantified and indicated below each panel. Numbers on the left indicate molecular mass in kD.

termed Prl-PrP[AV3]; Fig. 2). These results mirror the findings in vitro in two ways. First, PrP(AV3) and PrP(KH-II) are comparably potent at inducing $^{Ctm}$PrP, whereas PrP(A117V) was about half as potent. Second, the Prl signal largely normalizes the $^{Ctm}$PrP increase caused by the AV3 mutation. Thus, in both in vitro and cultured cell systems, signal sequence efficiency can modulate the amount of $^{Ctm}$PrP generation caused by an HD mutation.

### Signal sequence efficiency influences $^{Ctm}$PrP and neurodegeneration in vivo

Because HD mutants expressed in transgenic mice generate biochemically measurable $^{Ctm}$PrP and have pathological consequences (Hegde et al., 1998a, 1999), it should be possible to analyze signal sequence efficiency in vivo. We therefore reasoned that highly efficient signal sequences should reduce $^{Ctm}$PrP levels in the brain of an otherwise $^{Ctm}$PrP-producing HD mutation. Furthermore, if the proximal cause of neurodegeneration by the HD mutation is via generation of $^{Ctm}$PrP (as opposed to some other consequence of the mutation), then increasing signal sequence efficiency should also alleviate neurodegeneration. However, if $^{Ctm}$PrP is generated by a different mechanism in vivo, and differences in signal efficiency seen in vitro are inconsequential in vivo, then changing the signal sequence should not influence the behavior or consequences of an HD mutant. Thus, changing the native signal sequence of a PrP HD mutant to a different signal that in vitro analyses predict is more efficient should simultaneously allow two key hypotheses to be tested: one concerning the importance of signal sequence efficiency in the mechanism of PrP translocation, and another concerning the role of $^{Ctm}$PrP in mediating the downstream pathogenic consequences of certain inherited disease-associated PrP mutants.

A handful of signal sequences have been characterized and compared in vitro, and four HD mutants (AV3, KH-II, A117V, and N108I) have been examined in transgenic mice. In choosing among these, we decided on the Prl signal sequence and the artificial PrP(AV3) HD mutant for these studies for several reasons. First, the Prl signal sequence is perhaps the best studied mammalian signal sequence, and has been found to be highly efficient by numerous types of assays. Second, PrP(AV3) is a severely pathogenic mutant that leads to early onset disease phenotypes (by ~50 d of age) that even precluded generation of stable breeding transgenic lines (Hegde et al., 1998a). This means that rescue can be assessed without necessarily requiring prolonged observation times. Third, this mutation does not interfere with 3F4 antibody recognition (unlike KH-II or, to a lesser extent, N108I), which permits a reliable and sensitive assay for $^{Ctm}$PrP in brain extracts. A notable disadvantage of the AV3 mutation is that samples from the original transgenic animals described in Hegde et al. (1998a) are not available for direct comparison. However, analyses of brain tissue at that time had documented that, as expected from in vitro and cell culture studies, the proportion of PrP in the $^{Ctm}$PrP form for PrP(AV3) is very similar to that seen for PrP(KH-II), and roughly twofold higher than that seen with PrP(A117V) (Fig. S1 B). Importantly, archived samples from these key transgenic lines, termed PrP(KH-II)$_H$ and PrP(A117V)$_H$, were still available for comparison and could therefore serve as important standards for biochemical assays for $^{Ctm}$PrP levels. Thus, on balance, we felt the PrP(AV3) mutation would be the best test case for determining whether signal sequence efficiency is important to PrP biogenesis and disease in vivo.

A transgene coding for Prl-PrP(AV3) was introduced into mice (FVB background) and evaluated for expression, $^{Ctm}$PrP levels, and the development of neurodegenerative disease. To allow direct comparison to earlier studies (Hegde et al., 1998a, 1999), we used the same transgene vector as previously used to analyze PrP(AV3), PrP(KH-II), and PrP(A117V). This vector contains ~35 kB of the native PrP promoter and has been documented to precisely mirror the expression pattern of native PrP (Scott et al., 1989; Tremblay et al., 2007). To maximize the severity of any phenotype, PrP$^{+/+}$ mice were used because endogenous PrP was observed in earlier studies to exacerbate $^{Ctm}$PrP-mediated neurodegeneration (Stewart et al., 2005).

Three independent lines (designated with subscripts 6, 10, and 11) of Prl-PrP(AV3) were generated and analyzed. In contrast to earlier PrP(AV3) mice (Hegde et al., 1998a), Prl-PrP(AV3) mice were propagated readily and showed no gross abnormalities well into adulthood. Expression levels of the three mouse lines were analyzed by immunoblotting of total brain homogenates and compared with serial dilutions of homogenate from the PrP(A117V)$_H$ line of transgenic mice (Fig. 3 A).

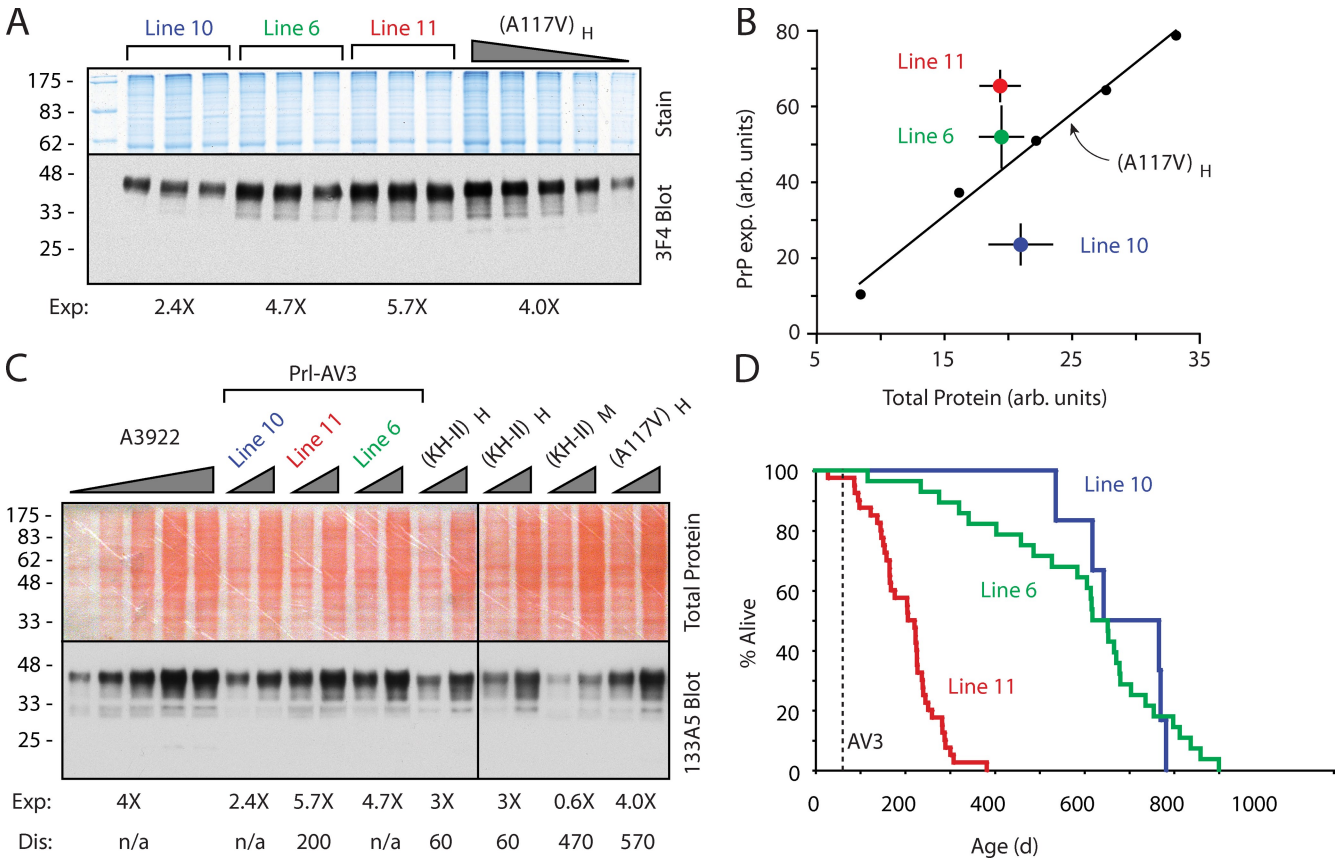


Figure 3. **Rescue from a disease-causing HD mutant by improving signal efficiency.** (A) Brain homogenates from three individual mice from each of the three Prl-PrP(AV3) transgenic lines were compared with serial dilutions of homogenate from PrP(A117V)$_H$ mice, which served as a standard. After SDS-PAGE, the upper portion of the gel was stained with colloidal coomassie blue, whereas the lower portion was immunoblotted using 3F4 antibody. (B) Quantification of two experiments, as in A, showing the PrP(A117V)$_H$ standards (black circles) and each transgenic line (mean ± SD; $n = 6$). Using an expression level of 4× for PrP(A117V)$_H$, the expression for lines 6, 10, and 11 were determined to be 2.4×, 4.7×, and 5.7×, respectively. (C) Expression levels of Prl-PrP(AV3) lines were compared with previously characterized mouse lines known to produce $^{Ctm}$PrP and develop neurodegeneration (Hegde et al., 1998a, 1999). The A3922 transgenic line, which expresses at 4×, served as a standard. Two amounts of each sample were loaded, and the blots were first stained for total protein with Ponceau S before immunoblotting with 13A5 antibody. The samples were run on two gels, with one set of samples (from PrP[KH-II]$_H$) duplicated on each gel to ensure that they were directly comparable. Below the lanes are the quantified expression levels and mean age of neurodegeneration taken from either this or earlier studies. "n/a" indicates that disease is not observed in these lines. The vertical black line indicates that intervening lanes have been spliced out. (D) Kaplan-Meier survival plots for the indicated transgenic mouse lines. The normal lifespan of this strain of mouse in our facility is ~600–800 d. The broken line indicates the age at which PrP(AV3) founders were observed to develop signs of disease (Hegde et al., 1998a). Numbers to the left of the blots in A and C indicate molecular mass in kD.

Previous quantification has shown that PrP(A117V)$_H$, which develops late onset neurodegenerative disease at ~570 d of age, expresses PrP at 4× the level found in normal hamster brain (Hegde et al., 1999). Relative to this standard, lines 6, 10, and 11 were found to express the transgene at 4.7 ± 0.4, 2.4 ± 0.4, and 5.7 ± 0.5, respectively (Fig. 3 B). These expression levels were as high or higher than PrP levels in several transgenic lines that developed $^{Ctm}$PrP-mediated disease in earlier studies (Fig. 3 C). Of note, earlier PrP(AV3) mice, all of which had succumbed to early onset disease without producing transgenic progeny, expressed the protein at between 1× and 4× (Hegde et al., 1998a). Thus, we were able to produce high-expressing transgenic lines from Prl-PrP(AV3).

Prl-PrP(AV3)$_6$ and Prl-PrP(AV3)$_{10}$ had normal lifespans of up to ~800 d (Fig. 3 D and Table I) and did not show gross clinical phenotypes indicative of neurodegeneration. This contrasts with earlier PrP(KH-II)$_H$, PrP(KH-II)$_M$, and PrP(A117V)$_H$ lines of transgenic mice, all of which consistently developed neurodegeneration at mean ages of 58, 472, and 572 d, respectively (Hegde et al., 1999). The comparison to PrP(KH-II)$_M$ and PrP(KH-II)$_H$ mice is particularly noteworthy because the AV3 and KH-II mutations have very similar effects on $^{Ctm}$PrP production in vitro, in cells, and in transgenic mice (Figs. 1, 2, and S1; Hegde et al., 1998a), and are comparably pathogenic in transgenic mice (Hegde et al., 1998a). Yet, Prl-PrP(AV3)$_6$ and Prl-PrP(AV3)$_{10}$ mice were phenotypically normal despite expressing the transgene at comparable or even considerably higher levels than either PrP(KH-II)$_M$ or PrP(KH-II)$_H$ mice (Fig. 3 C). In the most striking comparison, Prl-PrP(AV3)$_6$ mice express almost eightfold more mutant PrP than PrP(KH-II)$_M$ mice, yet remain disease free in comparison.

Prl-PrP(AV3) was not entirely without consequences, as line 11, which expresses the highest level of the transgene (~5.7×), developed signs of neurodegenerative disease and died between ~150 and 300 d. This was still considerably longer than the ~60 d course to disease of PrP(KH-II)$_H$, despite

Table I. **Characteristics of transgenic mice**

| Transgene[a] | Expression level[b] | $^{Ctm}$PrP in vitro[c] | $^{Ctm}$PrP in cells | $^{Ctm}$PrP in vivo[d] | Time to disease |
|---|---|---|---|---|---|
| | | % | % | | *d* |
| PrP(A3922) | 4.0× | ∼10 | <2 | <2 | >700 |
| PrP(KH-II)$_H$ | 3.0× | ∼30 | ∼10 | ∼10–20 | ∼60 |
| PrP(KH-II)$_M$ | 0.6× | ∼30 | ∼10 | ∼5–8 | ∼470 |
| PrP(A117V)$_H$ | 4.0× | ∼15 | ∼4 | ∼5–8 | ∼570 |
| PrP(AV3) | 1–4× | ∼35 | ∼10 | ∼10–20 | <60 |
| Prl-PrP(AV3)$_6$ | 4.7× | ∼15 | <2 | 2–5 | >600 |
| Prl-PrP(AV3)$_{10}$ | 2.4× | ∼15 | <2 | <2 | >600 |
| Prl-PrP(AV3)$_{11}$ | 5.7× | ∼15 | <2 | ∼5–8 | ∼200 |
| HuPrP(A117V)$_{36}$ | 2.4× | ∼15 | ∼4 | ND[e] | ∼560 |
| Opn-(A117V)$_{33}$ | 4.0× | ∼10 | <2 | ND[e] | >700 |

[a]The first five transgenic lines have been described previously (Hegde et al., 1998a, 1999).

[b]Relative to PrP levels in normal hamster (defined as 1×).

[c]Percentage of total PrP from a typical experiment. Exact amounts vary depending on experimental conditions and variations in the translation extract and ER microsomes. However, the relative relationships remain constant.

[d]Arbitrary units; determined by comparing the amount of the diagnostic 18-kD band generated by limited PK digestion to a serial dilution of total brain homogenate.

[e]Indicates not determined; the precise amounts could not be quantified because human PrP seems to behave slightly differently than rodent PrP in the limited PK digestion assay.

the fact that Prl-PrP(AV3)$_{11}$ expresses the transgene at nearly twofold higher levels and in the PrP$^{+/+}$ background. When taken together, our data suggest that replacing the wild-type PrP signal sequence with that from Prl renders the AV3 mutation considerably less pathogenic than it would be otherwise, permitting high-level expression (up to ∼4.7×) without obvious adverse consequences or a gross diminishment of lifespan.

To determine whether the phenotypic rescue effected by changing the signal sequence was caused by more efficient PrP translocation, brain tissue from Prl-PrP(AV3) mice was analyzed for $^{Ctm}$PrP using the limited protease digestion assay (Fig. 4 A). We found that all of the Prl-PrP(AV3) samples had lower total levels of $^{Ctm}$PrP than that seen with the PrP(KH-II)$_H$–positive control, which earlier studies have shown to generate similar levels of $^{Ctm}$PrP as PrP(AV3) (Fig. S1; Hegde et al., 1998a). It is worth emphasizing that equal amounts of brain homogenate were analyzed, meaning that total PrP levels in the Prl-PrP(AV3)$_6$ and Prl-PrP(AV3)$_{11}$ samples were 1.6- and 1.9-fold higher than in the PrP(KH-II)$_H$ sample. Thus, Prl-PrP(AV3) brain tissue not only contains less overall $^{Ctm}$PrP, but must necessarily be generating a considerably lower proportion of total PrP in the $^{Ctm}$PrP form relative to PrP(KH-II). This observation argues strongly that replacing the native PrP signal sequence on PrP(AV3) with that from Prl dramatically reduces $^{Ctm}$PrP production similar to in vitro and cultured cell analyses.

Overexposure of the blot revealed that $^{Ctm}$PrP in the higher-expressing Prl-PrP(AV3) lines was indeed detectable, and comparable to (line 11) or lower than (lines 6 and 10) that seen for PrP(A117V)$_H$ and PrP(KH-II)$_M$ (Fig. 4 A). Thus, there was a good general correlation between absolute amounts of $^{Ctm}$PrP as observed by this assay and development of neurodegeneration: PrP(KH-II)$_H$ shows very early onset disease and has the most $^{Ctm}$PrP; PrP(KH-II)$_M$, PrP(A117V)$_H$, and Prl-PrP(AV3)$_{11}$ have comparatively late-onset disease and clearly lower levels of $^{Ctm}$PrP; Prl-PrP(AV3)$_6$ and Prl-PrP(AV3)$_{10}$ have the least $^{Ctm}$PrP and do not develop obvious disease.

Because Prl-PrP(AV3)$_{11}$ develops disease at earlier ages than PrP(A117V)$_H$ mice (∼200 d versus ∼570 d), we compared their respective $^{Ctm}$PrP levels more closely (Fig. 4 B). Analysis of multiple animals showed ∼1.3-fold more $^{Ctm}$PrP in the Prl-PrP(AV3)$_{11}$ mice. Although this difference is rather modest, we believe it likely explains the more severe phenotype because earlier studies suggested a steep relationship between $^{Ctm}$PrP and age of disease onset. For example, the AV3 and KH-II mutations increase $^{Ctm}$PrP levels by only approximately twofold relative to A117V in vitro (Fig. 1 and Fig. S1; Hegde et al., 1998a), in cells (Fig. 2), and in transgenic mice (Fig. S1), yet are substantially more pathogenic and cause disease at both earlier ages and lower expression levels (Hegde et al., 1998a, 1999).

The quantification of $^{Ctm}$PrP in Prl-PrP(AV3)$_{11}$ relative to PrP(A117V)$_H$, combined with knowledge of the total PrP expression level in these mice, also allowed us to estimate the proportion of $^{Ctm}$PrP generated by Prl-PrP(AV3). As shown in the supplementary data of Chakrabarti and Hegde (2009), ∼6% of the PrP in PrP(A117)$_H$ mice is in the $^{Ctm}$PrP form. Given that Prl-PrP(AV3)$_{11}$ contains ∼1.3-fold more $^{Ctm}$PrP but ∼1.5-fold more total PrP, we conclude that a lower proportion of Prl-PrP(AV3) molecules are made as $^{Ctm}$PrP relative to the proportion generated by PrP(A117V) (∼5% compared with ∼6%). This conclusion is further supported by the observation that Prl-PrP(AV3)$_6$ has less overall $^{Ctm}$PrP than PrP(A117V)$_H$ despite expressing slightly higher total PrP (Fig. 4 A). Thus, the Prl signal substantially reduces the generation of $^{Ctm}$PrP by the AV3 mutation in transgenic mice to less than that seen for the A117V mutation. This reduction of $^{Ctm}$PrP corresponds to substantial attenuation of the neurodegenerative phenotype normally caused by the AV3 mutation.

### Rescue of a natural human disease mutant by improving signal sequence efficiency

The AV3 mutation is an artificial and exaggerated version of naturally occurring HD mutations that cause human disease. The studies on Prl-PrP(AV3) therefore represented a useful

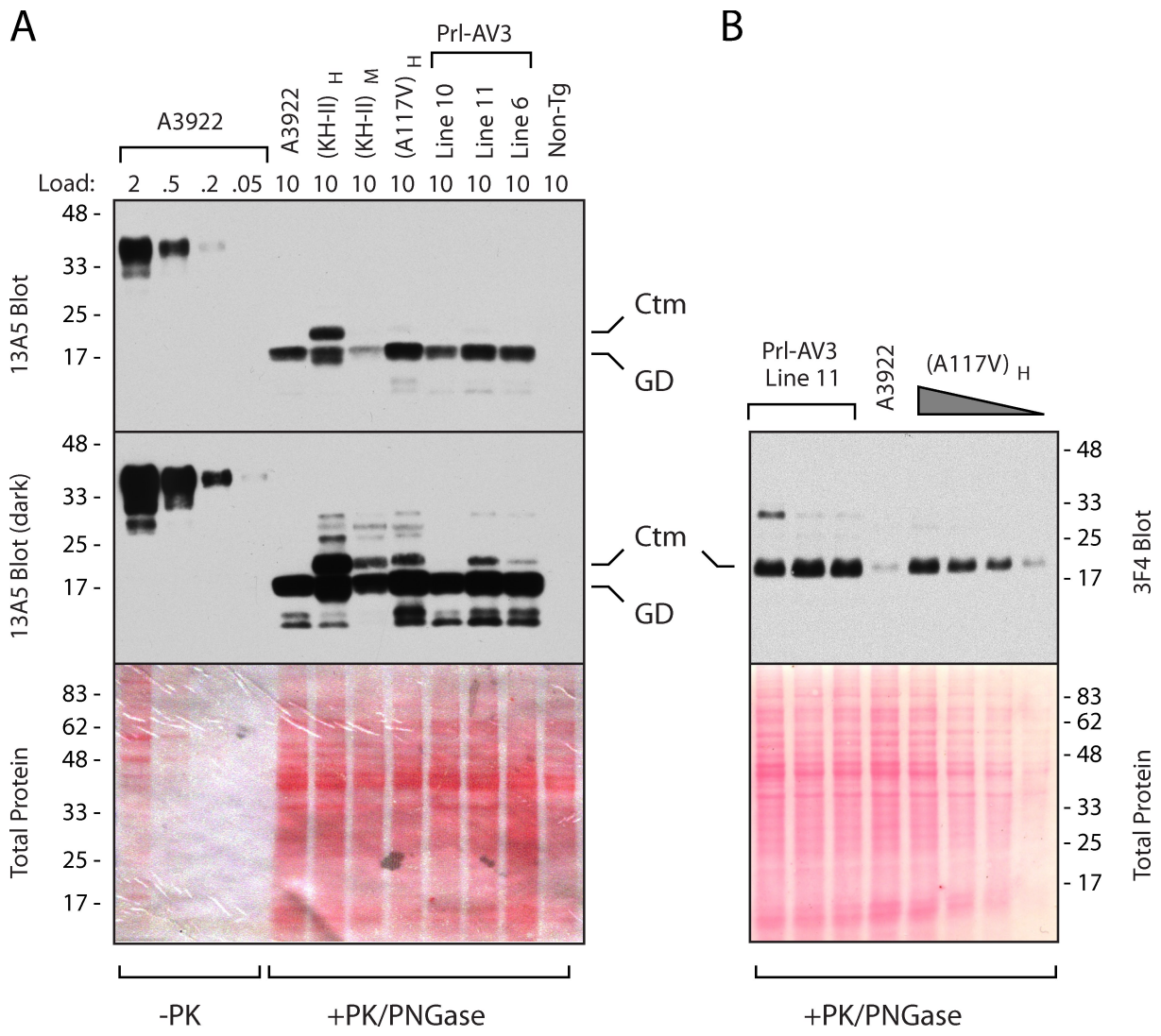


Figure 4. **Increased signal efficiency reduces $^{Ctm}$PrP levels in transgenic mice.** (A) Mouse brain homogenates from the indicated transgenic mice were subjected to limited PK digestion under "mild" conditions (see Materials and methods) and PrP detected by immunoblotting (two exposures, as well as total protein staining of the blot, are shown). The diagnostic $^{Ctm}$PrP-specific fragment and C-terminal GD that resists digestion under these conditions are indicated. The relative amounts of each sample loaded on the gel are indicated above the lanes. No signal was seen on the blot of samples digested under "harsh" conditions (not depicted). (B) Direct comparison of $^{Ctm}$PrP levels in three Prl-PrP(AV3) line 11 animals relative to PrP(A117V)$_H$. Quantification showed ~1.3× higher $^{Ctm}$PrP in Prl-PrP(AV3)$_{11}$. A3922 expresses wild-type PrP at 4×, and serves as a negative control. It contains very low, but detectable, levels of $^{Ctm}$PrP. Numbers to the sides of the blots indicate molecular mass in kD.

model system to analyze whether signal sequence inefficiency is involved in $^{Ctm}$PrP production in vivo, and to determine if $^{Ctm}$PrP has a causative role in neurodegenerative disease. Two key observations from in vitro analyses suggest that this model system can likely be generalized to natural HD mutations. First, each of the HD mutations, regardless of where within the HD they are located, are similarly reduced in their $^{Ctm}$PrP production by the Prl signal sequence (Fig. 1 C). Second, other efficient signal sequences can have the same effects as the Prl signal in reducing $^{Ctm}$PrP of HD mutations (Kim et al., 2002; Kim and Hegde, 2002), which suggests that the Prl signal is not unique. Thus, although based on experiments in heterologous in vitro systems, it seemed plausible to extrapolate our in vivo findings with Prl-PrP(AV3) and hypothesize that natural HD mutations generate disease-inducing $^{Ctm}$PrP because of signal sequence inefficiency, and hence can be rescued by an efficient signal.

To test this idea directly, we sought to analyze the human A117V mutant, which has successfully been modeled in transgenic mice (Hegde et al., 1999). This, however, posed some experimental limitations (hence the reason for initially focusing on the more tractable AV3 mutant). First, because the A117V mutation causes a relatively late-onset disease, any rescue would necessarily be modest because normal aging phenotypes and death will occur at only slightly later times. In fact, a rescue effect may be most apparent simply as the ability to express higher levels of the transgene without phenotypic consequences. Second, cell culture experiments suggest that the limited proteinase K (PK) digestion assay for analyzing $^{Ctm}$PrP is not as robust for human PrP (HuPrP) as with rodent PrP (unpublished data). For reasons that are not entirely clear, the subtle difference in conformation between $^{Ctm}$PrP and other PrP forms is not as readily maintained for HuPrP in detergent lysates, making

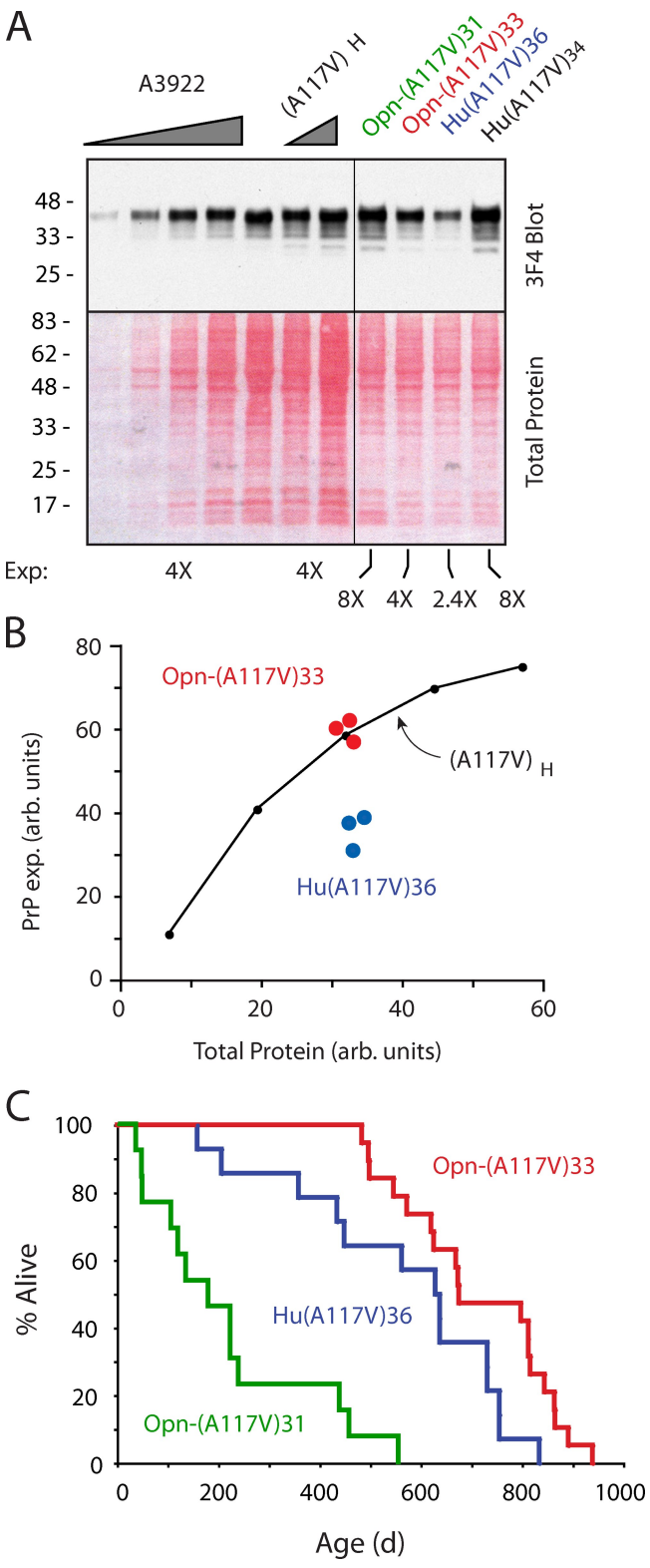


Figure 5. **Effect of improving signal efficiency on a human disease-causing HD mutant.** (A) Analysis of expression levels for the indicated transgenic mice using serial dilutions of the A3922 mouse as a standard. The blot was first stained for total protein with Ponceau S, followed by immunodetection with 3F4. All samples were analyzed on the same gel and are shown from the same exposure. The black vertical line indicates the position where an irrelevant lane was spliced out of the image. Numbers to the left indicate molecular mass in kD. (B) Quantification of expression levels in the indicated transgenic lines relative to PrP(A117V)$_H$ standards. Individual data points are shown. From this experiment, we calculated that HuPrP(A117V)$_{36}$ expresses at 2.4 ± 0.3×, whereas Opn-HuPrP(A117V)$_{33}$ expresses at 4 ± 0.2×. (C) Kaplan-Meier survival plots for the indicated transgenic mouse lines. The data for HuPrP(A117V)$_{36}$ was compared with Opn-HuPrP(A117V)$_{33}$ using the log-rank test and found to be statistically different (P = 0.02).

it quite difficult to detect $^{Ctm}$PrP and even harder to see small differences. And finally, A117V generates a rather small proportion of total PrP as $^{Ctm}$PrP (only ∼4–6%), making its further reduction more challenging to assess.

These potential obstacles notwithstanding, we generated transgenes for HuPrP(A117V) and a version of HuPrP(A117V) containing the signal sequence from the hormone osteopontin (termed Opn-HuPrP[A117V]). Earlier studies have shown that the Opn signal sequence is more efficient than the PrP signal (Kim et al., 2002; Levine et al., 2005), that it can improve PrP translocation in cell culture (Rane et al., 2004), and that it can reduce $^{Ctm}$PrP levels of HuPrP(A117V) to near wild-type levels in vitro (Kim and Hegde, 2002). Introduction of these transgenes into the FVB strain of PrP$^{+/+}$ mice generated several founders, the progeny of which were analyzed for expression levels (Fig. 5, A and B). Lines 34 and 36 of HuPrP(A117V) expressed the transgene at 8× and 2.4×, respectively. Of these, line 34 could not be analyzed further because the F1 progeny showed erratic behavioral abnormalities such as hyperactivity and locomotor problems that prevented their further breeding and expansion. We therefore focused on HuPrP(A117V)$_{36}$, which generated a colony of mice that were then observed throughout their lifetimes. Opn-HuPrP(A117V) also produced two lines whose expression levels were 4× (line 33) and 8× (line 31), both of which produced sufficient animals for observation and analysis. Line 31, which developed various phenotypes and died prematurely (Fig. 5 C), was not considered in detail because overexpression of even wild-type PrP at these levels causes an atypical disease that confounds analyses (Westaway et al., 1994; Chiesa et al., 2008). This left HuPrP(A117V)$_{36}$ and Opn-HuPrP(A117V)$_{33}$ for comparative phenotypic analyses.

Similar to previous studies overexpressing rodent PrP(A117V) in mice (Hegde et al., 1999; Yang et al., 2009), HuPrP(A117V)$_{36}$ displayed a slightly shortened mean lifespan of ∼560 d relative to the usual ∼600–800 d lifespan expected for our mouse facility (Fig. 5 C). In contrast, Opn-HuPrP(A117V)$_{33}$, which was produced at the same time, maintained in the same facility, and characterized in parallel, had a normal ∼710 d mean lifespan (Fig. 5 C). Although this difference in overall lifespan is rather modest, it was statistically significant (P = 0.02) using the log-rank test for evaluating survival data (Peto and Peto, 1972). Furthermore, the effect is actually the most it could have been given the mean ∼2-yr lifespan of normal FVB mice in our facility and elsewhere. Indeed, although large numbers of nontransgenic mice were not systematically maintained for their entire lifetimes because of space and cost constraints, we have not observed any mice living longer than the Opn-HuPrP(A117V)$_{33}$ line. In addition to this modest lifespan increase, there are several further observations that

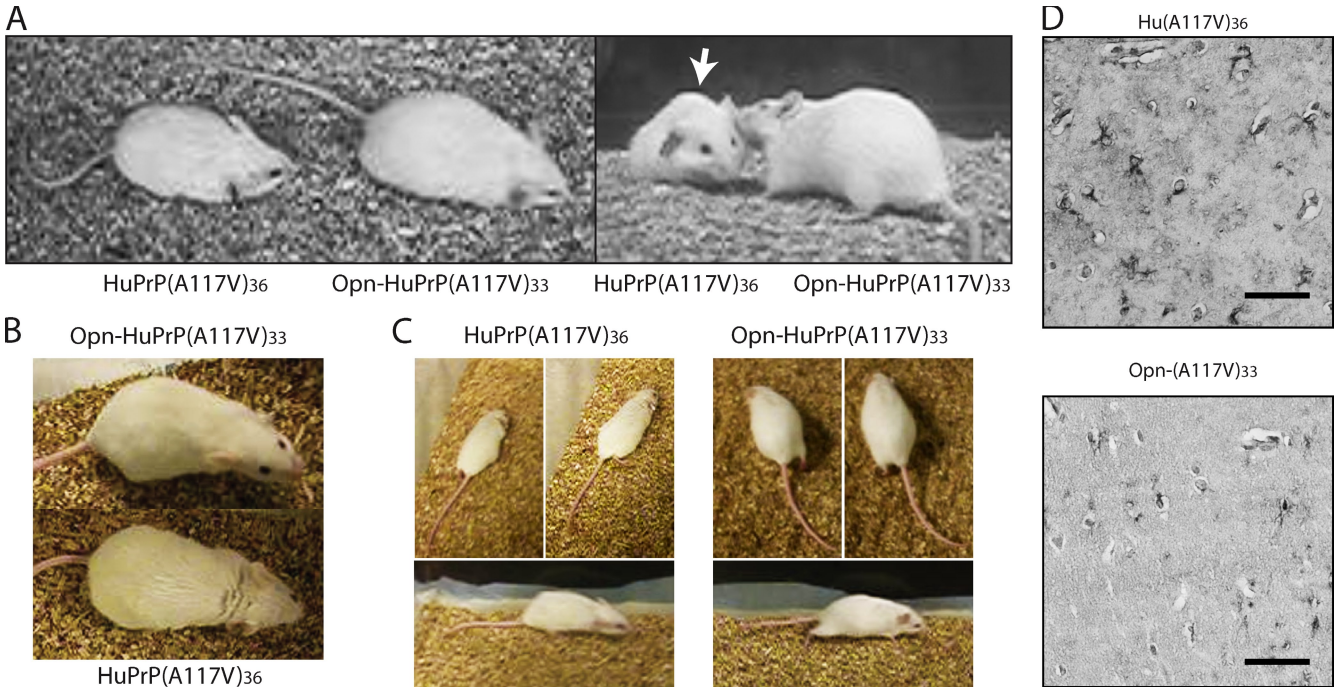


Figure 6. **Phenotypic rescue in transgenic mice upon improving signal efficiency.** (A) The smaller size of HuPrP(A117V)$_{36}$ mice often seen at older ages (which is indicative of some wasting) is not seen for Opn-HuPrP(A117V)$_{33}$. Some HuPrP(A117V)$_{36}$ mice also show kyphosis (hunched posture; arrow). (B) The rough hair coat in HuPrP(A117V)$_{36}$ mice, often an indicator of reduced grooming activity, is not seen in Opn-HuPrP(A117V)$_{33}$. (C) Evidence of hind limb weakness in HuPrP(A117V)$_{36}$ mice, but not in Opn-HuPrP(A117V)$_{33}$. The top two images in each panel show successive steps during normal walking. The bottom images show side views. Note that the HuPrP(A117V)$_{36}$ mouse is lower to the ground and the tail drags. In contrast, the Opn-HuPrP(A117V)$_{33}$ mouse keeps its posterior and tail elevated during walking. (D) Staining of brain sections from 2-yr-old HuPrP(A117V)$_{36}$ and Opn-HuPrP(A117V)$_{33}$ mice for astrogliosis using anti-GFAP antibody. A region of the hippocampus is shown. Bars, 50 µm.

indicated the Opn signal sequence had effected a rescue of the HuPrP(A117V) phenotype.

First, Opn-HuPrP(A117V)$_{33}$ expresses the transgene at higher levels than HuPrP(A117V)$_{36}$, with the difference corresponding to ~1.6 expression units (4× vs. 2.4×). This is not inconsequential given that an expression level difference of even smaller magnitude (5.7× vs. 4.7×) between Prl-PrP(AV3)$_{11}$ and Prl-PrP(AV3)$_{6}$ is sufficient to have clear phenotypic consequences. Similarly, PrP(KH-II)$_{H}$ and PrP(KH-II)$_{M}$ differ by ~2.4 expression units (~3× vs. 0.6×), which corresponded to a difference in disease development of ~60 d versus ~470 d. The fact that Opn-HuPrP(A117V)$_{33}$ discernibly increases lifespan despite substantially higher transgene expression compared to HuPrP(A117V)$_{36}$ is therefore notable.

Second, beginning at ~18 mo of age, HuPrP(A117V)$_{36}$ mice can be distinguished from Opn-HuPrP(A117V)$_{33}$ mice because the former, but the not latter, have a hunched posture, altered gait, and/or reduced hind-limb strength (Fig. 6, A–C). Many of the HuPrP(A117V)$_{36}$ mice also showed altered locomotor behavior including repeated circling, lethargy, and decreased responsiveness to external stimuli (Fig. S2). Such phenotypes were not seen in Opn-HuPrP(A117V)$_{33}$ mice even at ages >2 yr, which indicates a more substantive rescue than suggested by overall lifespan alone. Consistent with these differences in clinical phenotypes, immunohistochemistry showed slightly increased astrogliosis (detected as increased glial fibrillary acidic protein [GFAP] staining) in HuPrP(A117V)$_{36}$ relative to Opn-HuPrP(A117V)$_{33}$ (Fig. 6 D).

Third, although direct detection of $^{Ctm}$PrP for human PrP has not been possible yet because of technical constraints, there is nonetheless reason to believe that the Opn signal sequence has reduced the $^{Ctm}$PrP levels of the A117V mutation. This comes from the analysis of mahogunin, a cytosolic protein that can interact with $^{Ctm}$PrP via the cytosolically exposed N terminus (Chakrabarti and Hegde, 2009). We found that mahogunin immunoreactivity is altered in some brain regions of HuPrP(A117V)$_{36}$ mice, but is largely normal in Opn-HuPrP(A117V)$_{33}$ mice (Chakrabarti and Hegde, 2009), which suggests indirectly that cytosolic exposure of PrP was reduced by the Opn signal sequence.

Thus, when lifespan differences, clinical phenotypes, expression levels, and downstream effects on mahogunin are considered together, it is reasonable to suggest that Opn-HuPrP(A117V)$_{33}$ represents a phenotypically rescued version of HuPrP(A117V)$_{36}$. This conclusion is also most congruent with the observation that the Opn signal sequence reduces $^{Ctm}$PrP levels of HuPrP(A117V) to near wild type in vitro. Because two different HD pathogenic mutants (AV3 and A117V) were rescued by two different efficient signal sequences (from Prl and Opn), we believe that the phenotypic effects can confidently be attributed to a reduction of $^{Ctm}$PrP generation by improving native PrP signal sequence efficiency.

## Discussion

Our results suggest that protein translocation into the ER of a native protein in vivo is not necessarily maximally efficient.

We estimate that the failed translocation rate of wild-type PrP in physiologically appropriate cell types in vivo is roughly ∼10%, which is consistent with earlier in vitro and cell culture measurements (Kim et al., 2002; Rane et al., 2004; Levine et al., 2005; Kang et al., 2006). This means that the PrP signal sequence has substantial room for improvement in efficiency, as indicated by the striking consequences of the model Prl signal, which appears to be ∼96–98% efficient. These findings may be generally applicable to many other secretory proteins because both the sequence features (length, hydrophobicity, amino acid composition, and general domain structure) and functional properties (efficiency and interaction with translocon factors) of the PrP signal are rather typical of many ER targeting signals.

Indeed, several other signal sequences in their native context (e.g., from calreticulin [Shaffer et al., 2005], $p58^{IPK}$ [Rutkowski et al., 2007], and corticotropin-releasing factor receptor [Kang et al., 2006]) seem to be less than optimally efficient as judged by the ability of the Prl signal to improve translocation in vitro and/or in cells. Thus, around 5–10% of many secretory and membrane proteins might be constitutively mislocalized, presumably requiring their rapid degradation by the proteasome. Conversely, reduced proteasome activity, a feature of many diseases as well as normal aging (Chondrogianni and Gonos, 2005), may partially stabilize nontranslocated proteins. Similar to PrP (Ma et al., 2002), failed translocation of other proteins such as amyloid precursor protein and calreticulin can have biological effects in the cytosol (Anandatheerthavarada et al., 2003; Shaffer et al., 2005). Thus, the normally minor and transient nontranslocated population of several proteins could become physiologically or pathologically important under certain conditions.

For PrP, signal sequence insufficiency appears to play a direct role in at least a subset of familial diseases. Generation of disease-associated $^{Ctm}$PrP by HD mutations depends on the slight but measurable inefficiency of the PrP signal sequence. Both the disease phenotype and $^{Ctm}$PrP can be attenuated by improving signal sequence efficiency, strongly arguing for $^{Ctm}$PrP produced by these mutations as a primary pathogenic molecule. Thus, PrP HD mutants do not appear to be intrinsically toxic per se; instead, it is the consequence of the mutation for PrP localization that seems to be the key event in causing the disease phenotype. This explains how a pathogenic mutation (e.g., HuPrP[A117V]) can be rendered nonpathogenic by making second-site changes to a part of the open reading frame that is not even part of the final protein.

When combined with earlier observations that increased generation of nontranslocated PrP (by weakening or deleting the signal sequence) can cause neurodegeneration (Ma et al., 2002; Rane et al., 2008), it appears that prolonged or increased cytosolic exposure of PrP as either cyPrP or $^{Ctm}$PrP is especially detrimental in vivo. This could arise by any of several mechanisms including reduced PrP translocation during ER stress (Kang et al., 2006; Orsi et al., 2006), decreased proteasomal activity during prion infection and/or aging (Chondrogianni and Gonos, 2005; Kristiansen et al., 2007), mutations that lead to increased $^{Ctm}$PrP (Hegde et al., 1998a), or a combination of these effects. Thus, there may be multiple different mechanisms, all of which involve signal sequence inefficiency, that lead to the common detrimental endpoint of PrP mislocalization (Chakrabarti et al., 2009). Our recent finding that cytosolically mislocalized PrP interacts with and disturbs the function of the E3 ubiquitin ligase mahogunin provides at least one mechanistic basis for the downstream consequences of cyPrP exposure (Chakrabarti and Hegde, 2009).

Finally, it is worth considering why, if cytosolic mislocalization is detrimental, PrP has evolved to contain a less than maximally efficient signal sequence. One answer to this question may have to do with the finding that a suboptimal signal sequence is more easily modulated by trans-acting factors (Fons et al., 2003; Kang et al., 2006; Hegde and Kang, 2008), thereby providing the cell more flexibility. Indeed, the "weak" PrP signal sequence is beneficial and protective during ER stress because it facilitates reduced translocation into the ER, thereby preventing PrP aggregation in the secretory pathway (Kang et al., 2006). Thus, it may be that the potential advantages of a suboptimal but regulatable signal sequence outweigh the exceedingly low risk of adverse post-reproductive consequences represented by very rare inherited HD mutants and other PrP-mediated disorders.

## Materials and methods

### Antibodies

A 3F4 mouse monoclonal antibody against PrP (Covance) in the form of ascites was used at 1:10,000 dilution in Western blots. The 13A5 monoclonal antibody against PrP has been described previously (Rogers et al., 1991) and was used at 1:10,000 for blotting. Anti-GFAP rabbit polyclonal antibody was obtained from Novus Biologicals and diluted 1:1,000 for immunohistochemistry.

### Description of transgenes

The homozygous A3922 line of transgenic mice has been described previously (Hegde et al., 1998a), and expresses wild-type Syrian hamster PrP (SHaPrP) at ∼4× the level of that found in normal hamster brain. PrP(KH-II) describes a mutation in which residues 110 and 111 of SHaPrP are mutated to isoleucines (Hegde et al., 1998a). The "H" and "M" transgenic lines of PrP(KH-II) have been characterized previously in the FVB/$PrP^{-/-}$ background, and have been shown to develop neurodegeneration at ∼60 and ∼470 d, respectively (Hegde et al., 1998a, 1999). They typically died or were sacrificed within a few days after obvious symptoms were documented. $PrP(A117V)_H$ is a transgenic line expressing an alanine-to-valine change at position 117 in SHaPrP (Hegde et al., 1999). Expression levels are exactly the same as A3922. PrP(AV3) has been described previously, and when expressed as a transgene, causes early onset neurodegenerative disease (Hegde et al., 1998a). Multiple individual founder animals have been characterized, but none were stably established into breeding colonies. Disease was seen in animals with expression levels ranging from 1× to 4×. The Prl-PrP(AV3) construct was made by replacing the signal sequence and cleavage site (residues 1–25 of PrP) with the corresponding region (residues 1–33) of bovine preprolactin. Exchanging just the signals (residues 1–22 of PrP with residues 1–30 of Prl) caused somewhat heterogeneous signal cleavage in vitro. Thus, to ensure uniformity of signal cleavage, the signal and cleavage sites were exchanged. HuPrP(A117V) is human PrP containing the A117V mutation. Opn-HuPrP(A117V) contains the Opn signal sequence (residues 1–16) in place of the PrP signal (residues 1–22). In this case, signal cleavage heterogeneity was not observed, and previous analyses showed cleavage to be occurring at the expected position (Rane et al., 2004).

### Transgenic mouse production and analysis

The open reading frames coding for the indicated PrP constructs were subcloned into the Cos-tet cosmid containing ∼35 kb of the native PrP promoter (Hegde et al., 1998a) and expressed as transgenes in FVB mice. To maximize the severity of the phenotype (if any) caused by $^{Ctm}$PrP, the new

transgenic lines were made in the $PrP^{+/+}$ background because this was shown previously to accelerate $^{Ctm}$PrP-mediated neurodegeneration (Stewart et al., 2005). Thus, the fact that Prl-PrP(AV3) in the $PrP^{+/+}$ background is far less pathogenic than PrP(AV3) in the $PrP^{-/-}$ background is even more remarkable. Transgenic animal production, genotyping, and maintenance was performed as described previously (Hegde et al., 1998a). Animals were observed at least twice weekly, and any abnormal phenotypes were noted. In particular, unusual size, locomotor activity, gait, seizure, hair appearance, and body habitus, all symptoms that have been previously observed in mouse models of PrP-mediated neurodegeneration, were noted. Animals showing symptoms continued to be maintained to assess lifespan, except in cases where the veterinarian deemed them in severe distress, at which point they were sacrificed. In the Kaplan-Meier plots for lifespan, all deaths (including unexplained ones) were included except those in which animals were sacrificed prematurely for experiments or the rare instances where the reason could be attributed to unrelated causes such as wound infection or tumor. Statistical differences among lifespan curves were evaluated by the log-rank test (Peto and Peto, 1972) using the statistical package "R" (http://www.r-project.org/). In instances where the difference is visually obvious, exact p-values are not given but were all found to be $<10^{-4}$. The more modest difference between $HuPrP(A117V)_{36}$ and $Opn\text{-}HuPrP(A117V)_{33}$ was statistically significant at $P = 0.02$. Histological analysis for astrogliosis was performed on formalin-fixed paraffin sections of brain tissue with anti-GFAP polyclonal antibody and Vectastain ABC development reagents (Vector Laboratories), according to the manufacturer's instructions. Sections were subsequently counterstained with hematoxylin and mounted with mounting medium (Vectamount; Vector Laboratories). Brightfield imaging was performed using an upright microscope (Eclipse E600) and a 20×, 0.75 NA, air objective (all from Nikon). Images were captured using a digital camera (DXM1200F; Nikon) with the accompanying software. The images were imported as 8-bit TIFF images into Photoshop (Adobe), where they were subsequently cropped as needed, and incorporated into figures prepared using Illustrator (Adobe).

### Biochemical analyses

In vitro translocation assays, analyses of $^{Ctm}$PrP in cultured cells, and analyses of $^{Ctm}$PrP in mouse brain have been described previously (Hegde et al., 1998a). As detailed before (Hegde et al., 1998a), $^{Ctm}$PrP is partially resistant to PK digestion under "mild" conditions: 0.25 mg/ml PK for 60 min on ice in buffer containing 1% Triton X-100. $^{Ctm}$PrP generates a C-terminal fragment (residues ~105–231) which, upon deglycosylation, migrates at ~18 kD. In contrast, only residues ~125–231 of normal cellular PrP (the region that is structured in nuclear magnetic resonance studies) is resistant to digestion under these conditions. Both of these fragments are fully digested under the "harsh" conditions usually used to detect transmissible $PrP^{Sc}$ or PrP-res (0.1 mg/ml for 60 min at 37°C in buffer containing 0.5% Triton X-100 and 0.5% deoxycholate). Expression levels of PrP in the transgenic lines were quantified by running different amounts of total brain homogenate on the same gel as serial dilutions of a standard line (either A3922 or $PrP[A117V]_H$, both of which express PrP at 4×), and analyzed by immunoblotting with either the 3F4 or 13A5 monoclonal antibodies (neither of which detects endogenous mouse PrP). Total protein was judged by either cutting the top portion of the gel before transfer and staining with colloidal coomassie blue (e.g., Fig. 3 A) or by staining the blot with Ponceau S. At the amounts loaded and the exposures analyzed, quantification of protein and PrP levels were close to linear (e.g., Fig. 3 B and Fig. 5 B). At least three animals were analyzed to derive the estimate of expression levels. Note that all blots were stained with Ponceau S to confirm uniform transfer and equal loading. Images were digitized using a flatbed scanner in transmitted (for autorads and gels) or reflective (for stained blots) modes, and saved as raw 8-bit TIFF files. Figures were prepared using Photoshop and Illustrator software. Quantifications of stained or blotted images were performed using National Institutes of Health ImageJ. Serial dilutions were always included on gels to confirm that any quantification was in the linear range of the exposure chosen.

### Online supplemental material

Fig. S1 shows a comparative analysis of mutant PrP translocation in vitro and in vivo. Fig. S2 shows that locomotor phenotypes of HuPrP(A117V) mice are rescued by the Opn signal. Online supplemental material is available at http://www.jcb.org/cgi/content/full/jcb.200911115/DC1.

We are grateful to Y. Abebe for expert animal care and to N. Hegde for making some of the constructs. R.S. Hegde and N.S. Rane conceived the project and designed the experiments. N.S. Rane performed most of the experiments with contributions from R.S. Hegde and O. Chakrabarti. L. Feigenbaum generated transgenic mice. N.S. Rane, O. Chakrabarti, and R.S. Hegde interpreted the results. R.S. Hegde wrote the paper.

This work was supported by the Intramural Research Programs of the National Institute of Child Health and Human Development and the National Cancer Institute at the National Institutes of Health. The authors declare no competing financial interests.

Submitted: 20 November 2009
Accepted: 19 January 2010

## References

Anandatheerthavarada, H.K., G. Biswas, M.A. Robin, and N.G. Avadhani. 2003. Mitochondrial targeting and a novel transmembrane arrest of Alzheimer's amyloid precursor protein impairs mitochondrial function in neuronal cells. *J. Cell Biol.* 161:41–54. doi:10.1083/jcb.200207030

Belin, D., S. Bost, J.D. Vassalli, and K. Strub. 1996. A two-step recognition of signal sequences determines the translocation efficiency of proteins. *EMBO J.* 15:468–478.

Besemer, J., H. Harant, S. Wang, B. Oberhauser, K. Marquardt, C.A. Foster, E.P. Schreiner, J.E. de Vries, C. Dascher-Nadel, and I.J. Lindley. 2005. Selective inhibition of cotranslational translocation of vascular cell adhesion molecule 1. *Nature.* 436:290–293. doi:10.1038/nature03670

Chakrabarti, O., and R.S. Hegde. 2009. Functional depletion of mahogunin by cytosolically exposed prion protein contributes to neurodegeneration. *Cell.* 137:1136–1147. doi:10.1016/j.cell.2009.03.042

Chakrabarti, O., A. Ashok, and R.S. Hegde. 2009. Prion protein biosynthesis and its emerging role in neurodegeneration. *Trends Biochem. Sci.* 34:287–295. doi:10.1016/j.tibs.2009.03.001

Chiesa, R., P. Piccardo, E. Biasini, B. Ghetti, and D.A. Harris. 2008. Aggregated, wild-type prion protein causes neurological dysfunction and synaptic abnormalities. *J. Neurosci.* 28:13258–13267. doi:10.1523/JNEUROSCI.3109-08.2008

Chondrogianni, N., and E.S. Gonos. 2005. Proteasome dysfunction in mammalian aging: steps and factors involved. *Exp. Gerontol.* 40:931–938. doi:10.1016/j.exger.2005.09.004

Donne, D.G., J.H. Viles, D. Groth, I. Mehlhorn, T.L. James, F.E. Cohen, S.B. Prusiner, P.E. Wright, and H.J. Dyson. 1997. Structure of the recombinant full-length hamster prion protein PrP(29-231): the N terminus is highly flexible. *Proc. Natl. Acad. Sci. USA.* 94:13452–13457. doi:10.1073/pnas.94.25.13452

Drisaldi, B., R.S. Stewart, C. Adles, L.R. Stewart, E. Quaglio, E. Biasini, L. Fioriti, R. Chiesa, and D.A. Harris. 2003. Mutant PrP is delayed in its exit from the endoplasmic reticulum, but neither wild-type nor mutant PrP undergoes retrotranslocation prior to proteasomal degradation. *J. Biol. Chem.* 278:21732–21743. doi:10.1074/jbc.M213247200

Fons, R.D., B.A. Bogert, and R.S. Hegde. 2003. Substrate-specific function of the translocon-associated protein complex during translocation across the ER membrane. *J. Cell Biol.* 160:529–539. doi:10.1083/jcb.200210095

Garrison, J.L., E.J. Kunkel, R.S. Hegde, and J. Taunton. 2005. A substrate-specific inhibitor of protein translocation into the endoplasmic reticulum. *Nature.* 436:285–289. doi:10.1038/nature03821

Hegde, R.S., and H.D. Bernstein. 2006. The surprising complexity of signal sequences. *Trends Biochem. Sci.* 31:563–571. doi:10.1016/j.tibs.2006.08.004

Hegde, R.S., and S.W. Kang. 2008. The concept of translocational regulation. *J. Cell Biol.* 182:225–232. doi:10.1083/jcb.200804157

Hegde, R.S., J.A. Mastrianni, M.R. Scott, K.A. DeFea, P. Tremblay, M. Torchia, S.J. DeArmond, S.B. Prusiner, and V.R. Lingappa. 1998a. A transmembrane form of the prion protein in neurodegenerative disease. *Science.* 279:827–834. doi:10.1126/science.279.5352.827

Hegde, R.S., S. Voigt, and V.R. Lingappa. 1998b. Regulation of protein topology by trans-acting factors at the endoplasmic reticulum. *Mol. Cell.* 2:85–91. doi:10.1016/S1097-2765(00)80116-1

Hegde, R.S., P. Tremblay, D. Groth, S.J. DeArmond, S.B. Prusiner, and V.R. Lingappa. 1999. Transmissible and genetic prion diseases share a common pathway of neurodegeneration. *Nature.* 402:822–826. doi:10.1038/45574

Hsiao, K.K., C. Cass, G.D. Schellenberg, T. Bird, E. Devine-Gage, H. Wisniewski, and S.B. Prusiner. 1991. A prion protein variant in a family with the telencephalic form of Gerstmann-Sträussler-Scheinker syndrome. *Neurology.* 41:681–684.

Kang, S.W., N.S. Rane, S.J. Kim, J.L. Garrison, J. Taunton, and R.S. Hegde. 2006. Substrate-specific translocational attenuation during ER stress defines a pre-emptive quality control pathway. *Cell.* 127:999–1013. doi:10.1016/j.cell.2006.10.032

Kim, S.J., and R.S. Hegde. 2002. Cotranslational partitioning of nascent prion protein into multiple populations at the translocation channel. *Mol. Biol. Cell.* 13:3775–3786. doi:10.1091/mbc.E02-05-0293

Kim, S.J., R. Rahbar, and R.S. Hegde. 2001. Combinatorial control of prion protein biogenesis by the signal sequence and transmembrane domain. *J. Biol. Chem.* 276:26132–26140. doi:10.1074/jbc.M101638200

Kim, S.J., D. Mitra, J.R. Salerno, and R.S. Hegde. 2002. Signal sequences control gating of the protein translocation channel in a substrate-specific manner. *Dev. Cell.* 2:207–217. doi:10.1016/S1534-5807(01)00120-4

Kristiansen, M., P. Deriziotis, D.E. Dimcheff, G.S. Jackson, H. Ovaa, H. Naumann, A.R. Clarke, F.W. van Leeuwen, V. Menéndez-Benito, N.P. Dantuma, et al. 2007. Disease-associated prion protein oligomers inhibit the 26S proteasome. *Mol. Cell.* 26:175–188. doi:10.1016/j.molcel.2007.04.001

Levine, C.G., D. Mitra, A. Sharma, C.L. Smith, and R.S. Hegde. 2005. The efficiency of protein compartmentalization into the secretory pathway. *Mol. Biol. Cell.* 16:279–291. doi:10.1091/mbc.E04-06-0508

Lopez, C.D., C.S. Yost, S.B. Prusiner, R.M. Myers, and V.R. Lingappa. 1990. Unusual topogenic sequence directs prion protein biogenesis. *Science.* 248:226–229. doi:10.1126/science.1970195

Ma, J., and S. Lindquist. 2001. Wild-type PrP and a mutant associated with prion disease are subject to retrograde transport and proteasome degradation. *Proc. Natl. Acad. Sci. USA.* 98:14955–14960. doi:10.1073/pnas.011578098

Ma, J., R. Wollmann, and S. Lindquist. 2002. Neurotoxicity and neurodegeneration when PrP accumulates in the cytosol. *Science.* 298:1781–1785. doi:10.1126/science.1073725

Martoglio, B., and B. Dobberstein. 1998. Signal sequences: more than just greasy peptides. *Trends Cell Biol.* 8:410–415. doi:10.1016/S0962-8924(98)01360-9

Orsi, A., L. Fioriti, R. Chiesa, and R. Sitia. 2006. Conditions of endoplasmic reticulum stress favor the accumulation of cytosolic prion protein. *J. Biol. Chem.* 281:30431–30438. doi:10.1074/jbc.M605320200

Panegyres, P.K., K. Toufexis, B.A. Kakulas, L. Cernevakova, P. Brown, B. Ghetti, P. Piccardo, and S.R. Dlouhy. 2001. A new PRNP mutation (G131V) associated with Gerstmann-Sträussler-Scheinker disease. *Arch. Neurol.* 58:1899–1902. doi:10.1001/archneur.58.11.1899

Peto, R., and J. Peto. 1972. Asymptotically efficient rank invariant test procedures. *J. R. Stat. Soc. Ser. A Stat. Soc.* 135:185–207.

Prusiner, S.B., M.R. Scott, S.J. DeArmond, and F.E. Cohen. 1998. Prion protein biology. *Cell.* 93:337–348. doi:10.1016/S0092-8674(00)81163-0

Rane, N.S., J.L. Yonkovich, and R.S. Hegde. 2004. Protection from cytosolic prion protein toxicity by modulation of protein translocation. *EMBO J.* 23:4550–4559. doi:10.1038/sj.emboj.7600462

Rane, N.S., S.W. Kang, O. Chakrabarti, L. Feigenbaum, and R.S. Hegde. 2008. Reduced translocation of nascent prion protein during ER stress contributes to neurodegeneration. *Dev. Cell.* 15:359–370. doi:10.1016/j.devcel.2008.06.015

Rapoport, T.A. 2007. Protein translocation across the eukaryotic endoplasmic reticulum and bacterial plasma membranes. *Nature.* 450:663–669. doi:10.1038/nature06384

Riek, R., S. Hornemann, G. Wider, M. Billeter, R. Glockshuber, and K. Wüthrich. 1996. NMR structure of the mouse prion protein domain PrP(121-321). *Nature.* 382:180–182. doi:10.1038/382180a0

Riek, R., S. Hornemann, G. Wider, R. Glockshuber, and K. Wüthrich. 1997. NMR characterization of the full-length recombinant murine prion protein, mPrP(23-231). *FEBS Lett.* 413:282–288. doi:10.1016/S0014-5793(97)00920-4

Rodriguez, M.M., K. Peoc'h, S. Haïk, C. Bouchet, L. Vernengo, G. Mañana, R. Salamano, L. Carrasco, M. Lenne, P. Beaudry, et al. 2005. A novel mutation (G114V) in the prion protein gene in a family with inherited prion disease. *Neurology.* 64:1455–1457.

Rogers, M., D. Serban, T. Gyuris, M. Scott, T. Torchia, and S.B. Prusiner. 1991. Epitope mapping of the Syrian hamster prion protein utilizing chimeric and mutant genes in a vaccinia virus expression system. *J. Immunol.* 147:3568–3574.

Rutkowski, D.T., V.R. Lingappa, and R.S. Hegde. 2001. Substrate-specific regulation of the ribosome- translocon junction by N-terminal signal sequences. *Proc. Natl. Acad. Sci. USA.* 98:7823–7828. doi:10.1073/pnas.141125098

Rutkowski, D.T., S.W. Kang, A.G. Goodman, J.L. Garrison, J. Taunton, M.G. Katze, R.J. Kaufman, and R.S. Hegde. 2007. The role of p58IPK in protecting the stressed endoplasmic reticulum. *Mol. Biol. Cell.* 18:3681–3691. doi:10.1091/mbc.E07-03-0272

Scott, M., D. Foster, C. Mirenda, D. Serban, F. Coufal, M. Wälchli, M. Torchia, D. Groth, G. Carlson, S.J. DeArmond, et al. 1989. Transgenic mice expressing hamster prion protein produce species-specific scrapie infectivity and amyloid plaques. *Cell.* 59:847–857. doi:10.1016/0092-8674(89)90608-9

Shaffer, K.L., A. Sharma, E.L. Snapp, and R.S. Hegde. 2005. Regulation of protein compartmentalization expands the diversity of protein function. *Dev. Cell.* 9:545–554. doi:10.1016/j.devcel.2005.09.001

Stewart, R.S., and D.A. Harris. 2003. Mutational analysis of topological determinants in prion protein (PrP) and measurement of transmembrane and cytosolic PrP during prion infection. *J. Biol. Chem.* 278:45960–45968. doi:10.1074/jbc.M307833200

Stewart, R.S., and D.A. Harris. 2005. A transmembrane form of the prion protein is localized in the Golgi apparatus of neurons. *J. Biol. Chem.* 280:15855–15864. doi:10.1074/jbc.M412298200

Stewart, R.S., P. Piccardo, B. Ghetti, and D.A. Harris. 2005. Neurodegenerative illness in transgenic mice expressing a transmembrane form of the prion protein. *J. Neurosci.* 25:3469–3477. doi:10.1523/JNEUROSCI.0105-05.2005

Tateishi, J., T. Kitamoto, K. Doh-ura, Y. Sakaki, G. Steinmetz, C. Tranchant, J.M. Warter, and N. Heldt. 1990. Immunochemical, molecular genetic, and transmission studies on a case of Gerstmann-Sträussler-Scheinker syndrome. *Neurology.* 40:1578–1581.

Tremblay, P., E. Bouzamondo-Bernstein, C. Heinrich, S.B. Prusiner, and S.J. DeArmond. 2007. Developmental expression of PrP in the post-implantation embryo. *Brain Res.* 1139:60–67. doi:10.1016/j.brainres.2006.12.055

Voigt, S., B. Jungnickel, E. Hartmann, and T.A. Rapoport. 1996. Signal sequence-dependent function of the TRAM protein during early phases of protein transport across the endoplasmic reticulum membrane. *J. Cell Biol.* 134:25–35. doi:10.1083/jcb.134.1.25

von Heijne, G. 1985. Signal sequences. The limits of variation. *J. Mol. Biol.* 184:99–105. doi:10.1016/0022-2836(85)90046-4

Westaway, D., S.J. DeArmond, J. Cayetano-Canlas, D. Groth, D. Foster, S.L. Yang, M. Torchia, G.A. Carlson, and S.B. Prusiner. 1994. Degeneration of skeletal muscle, peripheral nerves, and the central nervous system in transgenic mice overexpressing wild-type prion proteins. *Cell.* 76:117–129. doi:10.1016/0092-8674(94)90177-5

Yang, W., J. Cook, B. Rassbach, A. Lemus, S.J. DeArmond, and J.A. Mastrianni. 2009. A new transgenic mouse model of Gerstmann-Sträussler-Scheinker syndrome caused by the A117V mutation of PRNP. *J. Neurosci.* 29:10072–10080. doi:10.1523/JNEUROSCI.2542-09.2009

Yedidia, Y., L. Horonchik, S. Tzaban, A. Yanai, and A. Taraboulos. 2001. Proteasomes and ubiquitin are involved in the turnover of the wild-type prion protein. *EMBO J.* 20:5383–5391. doi:10.1093/emboj/20.19.5383

Published



Rane et al., http://www.jcb.org/cgi/content/full/jcb.200911115/DC1

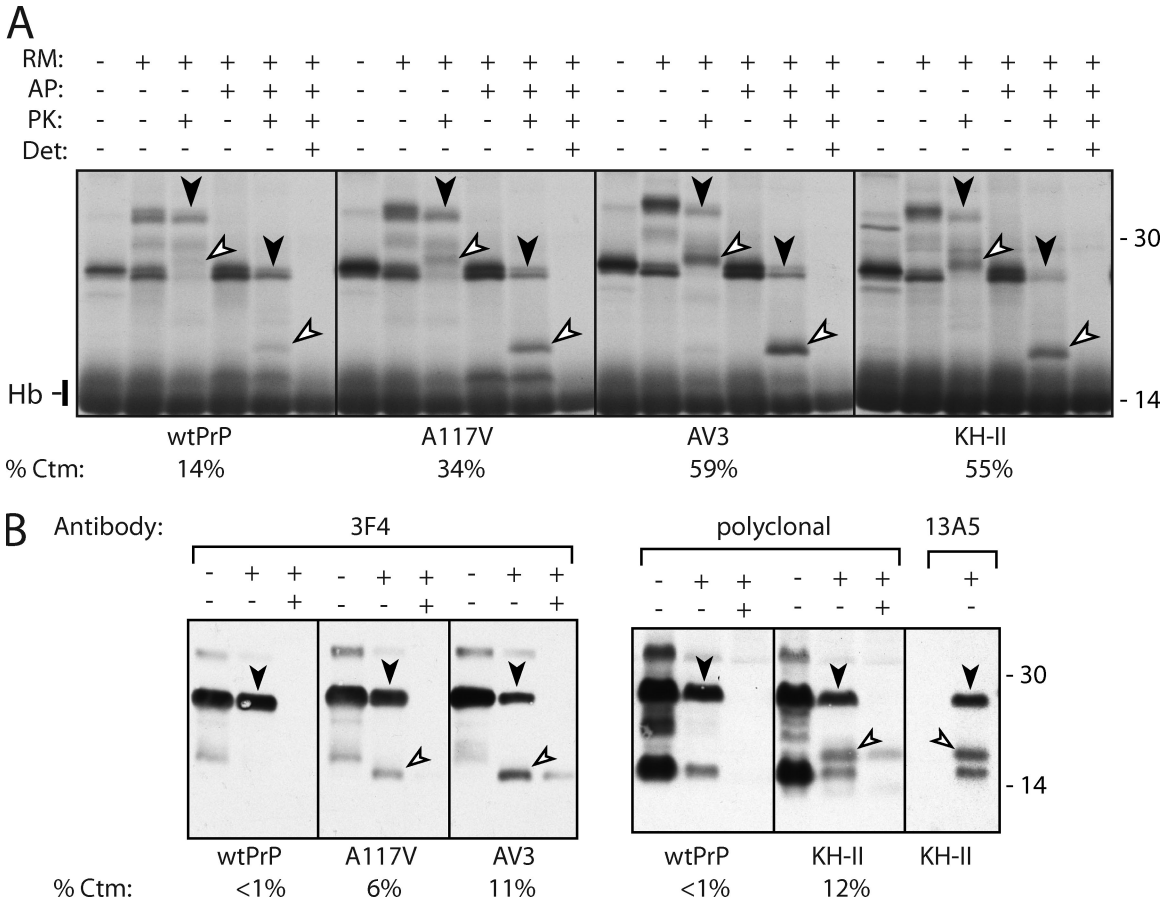


Figure S1. **Comparative analysis of key PrP mutants in vitro and in vivo.** (A) Wild-type PrP, PrP(A117V), PrP(AV3), and PrP(KH-II), all of hamster origin, were synthesized as $^{35}$S-labeled proteins in reticulocyte lysate and analyzed by a protease protection assay for translocation as before (Hegde et al., 1998. *Science*. 279:827–834). Translation reactions were performed with or without canine pancreatic rough microsomes (RM) in the absence or presence of a glycosylation acceptor peptide (AP) to inhibit glycosylation as indicated. After translation, samples were moved to ice and incubated with or without PK in the absence or presence of detergent (Det; 1% Triton X-100). The products were analyzed by SDS-PAGE, and the translated proteins were visualized by autoradiography. The position of endogenous hemoglobin, which gets labeled to some degree, is indicated (Hb). The fully protected product, indicative of sec-PrP, is marked with black arrowheads. In lane 3 of each sample, this product is glycosylated; in lane 5, it is not. The C-terminal fragment produced by proteolysis of CtmPrP is indicated by the white arrowheads. It is glycosylated in lane 3 and unglycosylated in lane 5. Note that in the presence of detergent, all products are digested under these conditions. The proportion of total synthesized PrP that is made in the CtmPrP form was quantified and is shown below the gels. The analysis in Fig. 1 C shows samples processed as in lane 5, which allows a facile comparison of CtmPrP levels among samples. (B) A crude microsome preparation from brain tissue taken from transgenic animals overexpressing wild-type PrP, PrP(A117V), PrP(AV3), or PrP(KH-II) was digested with PK in the absence or presence of detergent. The samples were then deglycosylated with peptide-*N*-glycosidase F and analyzed by SDS-PAGE and immunoblotting. The samples are from animals described in Hegde et al. (1998. *Science*. 279:827–834), and are transgenic line A3922 (wild-type PrP), PrP(A117V)H, and PrP(KH-II)H. The AV3 sample is from a founder animal because it could not be bred into a stable line due to illness. The left panel shows an immunoblot with the 3F4 antibody. The fully protected band (black arrowheads) is apparently in the lumen of the microsomes, whereas the 3F4-reactive fragment (white arrowheads) is generated by the transmembrane CtmPrP form. Note that this fragment resists digestion in brain tissue even in the presence of detergent, which forms the basis for a limited protease digestion assay for CtmPrP. PrP(KH-II) is not recognized by the 3F4 antibody, so this sample was probed with either a polyclonal antibody against whole PrP or the 13A5 antibody. With these antibodies, other bands representing endogenous PrP degradation intermediates (in the minus PK lanes) or the folded C-terminal GD that resists PK digestion are visualized. Quantification of CtmPrP levels as a percentage of total PrP is indicated below the gels. Note that in all systems (in vitro, cultured cells, and in brain), A117V generates more CtmPrP than wild type, but less than either AV3 or KH-II, which are roughly equal in their propensity to generate CtmPrP. Numbers to the right of the gel blots indicate molecular mass in kD.

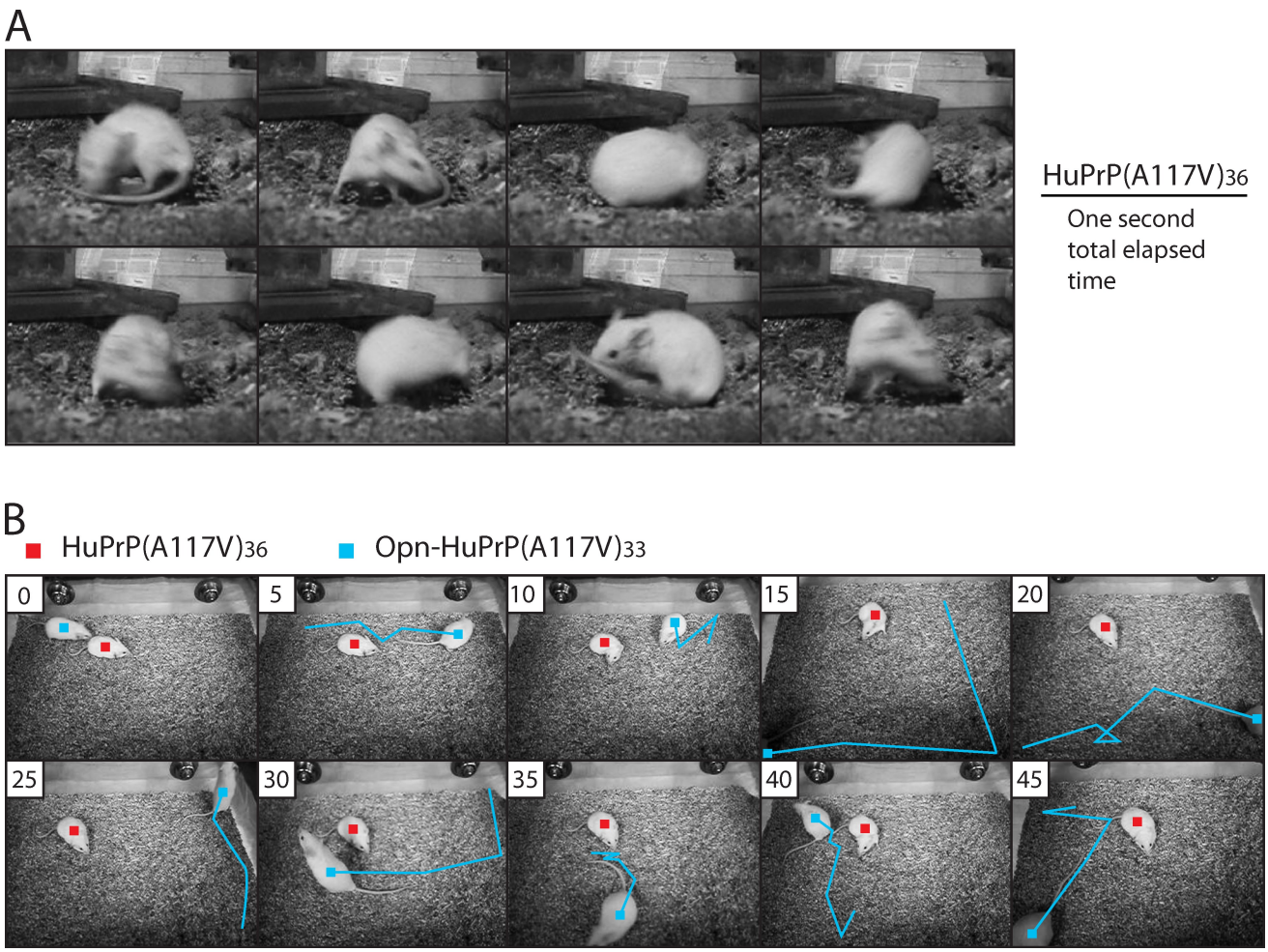


Figure S2. **Locomotor phenotypes of HuPrP(A117V) mice are rescued by the Opn signal.** (A) Rapid circling behavior seen in many HuPrP(A117V)36 mice. Shown are a succession of images spanning a total of 1 s. This animal continued with this behavior over the course of the entire 1-min movie, and showed repeated intermittent circling behavior throughout the day. The age of the animal is 22 mo. (B) Reduced activity seen in some HuPrP(A117V)36 mice but not Opn-HuPrP(A117V)33 mice. Shown are frames from a 45-s movie tracking the movements of the indicated transgenic mice. The HuPrP(A117V)36 mouse (red) barely moved, even after some prodding, whereas the Opn- HuPrP(A117V)33 mouse (blue) showed normal exploratory behavior. The blue lines trace the movement since the previous frame. The age of both mice was ~19 mo. The mice were placed in the observation cage and acclimated for ~10 min before recording the movie.